

# We are IntechOpen, the world's leading publisher of Open Access books Built by scientists, for scientists

6,900

Open access books available

186,000

International authors and editors

200M

Downloads

Our authors are among the

154

Countries delivered to

TOP 1%

most cited scientists

12.2%

Contributors from top 500 universities



WEB OF SCIENCE™

Selection of our books indexed in the Book Citation Index  
in Web of Science™ Core Collection (BKCI)

Interested in publishing with us?  
Contact [book.department@intechopen.com](mailto:book.department@intechopen.com)

Numbers displayed above are based on latest data collected.  
For more information visit [www.intechopen.com](http://www.intechopen.com)



# Fabrication of Apatite Films on Ti Substrates of Simple and Complicated Shapes by Using Stable Solutions of Ca Complex

*Chihiro Mochizuki, Mitsunobu Sato and Tohru Hayakawa*

## Abstract

Titanium (Ti) is known as the most popular implant materials. In addition, the coating technology of hydroxyapatite (HA) or carbonate-containing apatite (CA) on Ti substrates having various shapes has been interested from the viewpoint for improvement of implant's osteoconductivity. The fabrication of apatite coatings on metallic substrates has been investigated by several techniques. We developed novel wet processes using some stable solutions in which Ca complexes and phosphate ion dissolve simultaneously. The CA film can be deposited homogeneously on substrates, Ti plate and Ti fiber mesh, using a stable precursor solution involving a  $\text{Ca}^{2+}$  complex of ethylenediaminetetraacetic acid (EDTA). Another stable aqueous solution was prepared by the addition of phosphoric acid to a calcium hydrogen carbonate solution. The solution is adequate to be sprayed facilely onto a Ti plate by using an airbrush. It is important that the fabricated apatite films by the spray process have the characteristic network structures. The materials with these CA films are nontoxic and have the excellent bonding ability to bone tissues.

**Keywords:** apatite film, implant, Ca complex, chemical process

## 1. Introduction

Titanium (Ti) and its alloys are the most commonly used metal for the manufacture of orthopedic implants, while hydroxyapatite (HA), which is a calcium phosphate ceramic, is bioactive and biocompatible when used as a bone substitute. To improve the biocompatibility and mechanical properties of prostheses, calcium phosphate coatings on titanium surfaces are often investigated in order to combine the benefits of both the materials [1, 2]. In addition to HA, the deposition of other carbonate-containing apatite (CA) films on titanium substrates is interesting because of the resulting chemical resemblance to bone mineral [3]. For the coating method, physical vapor deposition (PVD) techniques such as ion plating [4], magnetron sputtering [5], and ion beam dynamic mixing [6] have been introduced to deposit thin calcium phosphate coatings on medical or oral implants. A plasma spray technique, which is a physical process, is currently the most widely used method for the deposition of calcium phosphate

coatings on Ti substrates [7–10]. However, plasma-sprayed calcium phosphate coatings have some shortcomings such as faster degradation and fatigue of the coating; moreover, their long-term clinical safety has been questioned [11–13]. On the other hand, Liu et al. [14] deposited a thin hydroxyapatite film on stainless steel using a water-based sol-gel technique. A dense and adhesive apatite coating can be produced through water-based sol-gel technology after short-term annealing at around 400°C in air. Kim et al. [15] used a sol-gel method to coat a fluoro-hydroxyapatite film on a zirconia substrate. The use of the sol-gel technique has the potential for applying uniform coatings to porous substrates. However, in the conventional sol-gel process, alkoxides are employed, and the rigorous exclusion of water from the system is essential for the synthesis and conservation of the precursor alkoxides and their solutions since the process is based on partial or complete hydrolysis of such metal alkoxides [16]. Furthermore, Leeuwenburgh et al. [17, 18] and Siebers et al. [19, 20] reported a CA coating produced using electrostatic spray deposition (ESD) that was originally developed to fabricate thick ceramic films for solid electrolytes [21]. Amorphous films deposited by ESD on a substrate heated to 470°C converted to crystalline CA films after heat treatment at temperatures above 700°C for 15 s in air. Additionally, Siebers et al. [22] assayed the cell proliferation, alkaline phosphatase activity, and osteocalcin concentration of the osteoblast-like cells of the CA coatings deposited by ESD.

This chapter focuses on the fabrication of apatite film on Ti substrate by chemical process used in the metal complexes. We prepared two coating solutions with sufficient concentrations of  $\text{Ca}^{2+}$  complex and  $\text{PO}_4^{3-}$  ion. CA film on Ti substrates fabricated by the solvent of one solution is ethanol, and another one is aqueous solution. Resultant films evaluated the characteristic and animal experimental.

## 2. Molecular precursor method for apatite coating on titanium substrates

### 2.1 Preparation of stable coating solution by molecular precursor method

The molecular precursor method (MPM) that was developed in our study is one of chemical processes for fabricating metal oxide and phosphate thin films [23–28]. This method is based on the design of metal complexes in coating solutions with excellent stability, homogeneity, miscibility, coatability, etc., which have many practical advantages. This is because metal complex anions with high stability can be generally dissolved in volatile solvents adequate to spin-coating, etc., by combining them with appropriate alkylamines *via* acid-base reaction. Furthermore, the resultant solutions can form excellent precursor films through various coating procedures. The precursor films involving metal complexes should be amorphous in order to obtain homogeneous films without crack and pinhole. Heat-treatment is usually employed to fabricate the desired metal oxide or phosphate films by eliminating the ligand in the metal complex and alkylamine in the precursor films. It is important that densification of the films during heat treatment occurs only in the vertical direction on the substrate.

The molecular precursor solution for the CA coating was obtained as an ethanol solution by adding diphosphate salt to a butylammonium salt of Ca complex with EDTA, which was isolated by the reaction of ethylenediamine-*N*, *N*, *N'*, *N'*-tetraacetic acid (EDTA) and  $\text{Ca}(\text{CH}_3\text{COO})_2 \cdot 2\text{H}_2\text{O}$  from the hot aqueous solution. The obtained solution was clear and stable.

The general procedure for preparing the molecular precursor solution is shown in **Figure 1** [29].

The abovementioned Ca complex was isolated as a white powder and characterized by elemental analysis, Fourier transform infrared (FT-IR), and thermogravimetry-differential thermal analysis (TG-DTA). **Figure 2** shows the FT-IR spectra of

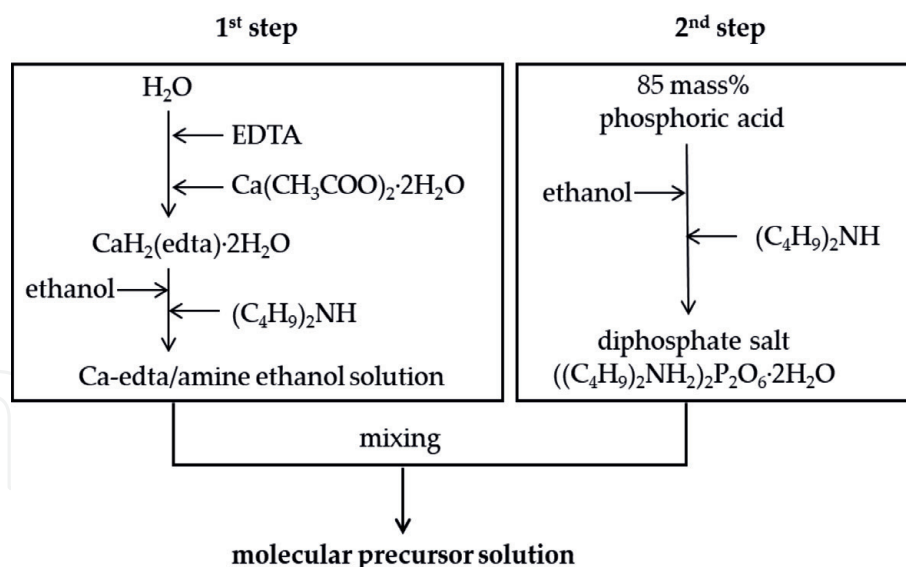


**Figure 1.**  
 Schematic of preparation of precursor solution.

the white compound. The characteristic peak assignable to carboxyl group can be observed at  $1620 \text{ cm}^{-1}$ . The peaks at  $1200$ ,  $2980$ , and  $3360 \text{ cm}^{-1}$  can be assigned to  $\text{H}_5\text{O}_2^+$  ion. **Figure 3** shows TG-DTA curves of the obtained white compound. The endothermic peak with the mass loss at  $235^\circ\text{C}$  can be assigned to the elimination of the coordinated water molecules. It was clarified by these results that the number of coordinated water is 2. The exothermic peak with the mass loss from  $324$  to  $464^\circ\text{C}$  corresponds to the combustion of EDTA. As a result, the chemical component of the isolated white powder was confirmed as  $(\text{H})(\text{H}_5\text{O}_2)[\text{Ca}(\text{edta})]$  and consistent to the elemental analysis.

The isolated Ca complex of EDTA is not soluble to ethanol, producing a suspended solution when the compound is added into the solvent. However, by the addition of dibutylamine to the suspended solution, a clear solution can be facilely obtained. In addition, the dibutylammonium salt of the Ca complex with EDTA produces an amorphous film on the Ti substrate by spin-coating before firing, under the presence of phosphate ion.

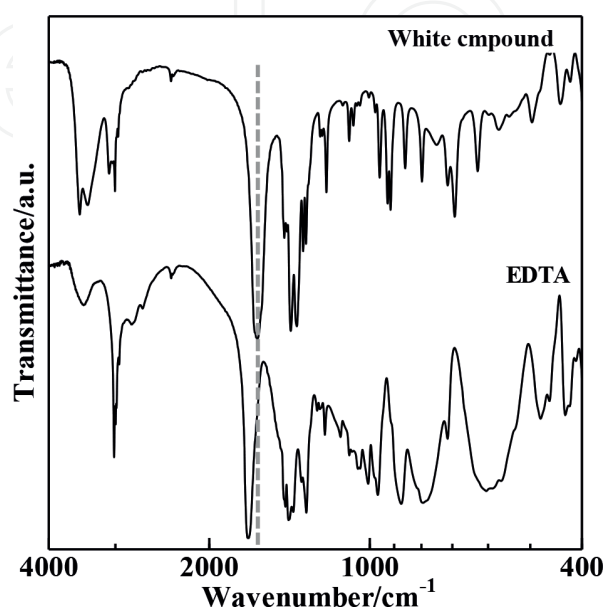


**Figure 2.**  
 FT-IR spectra of EDTA and white compound.

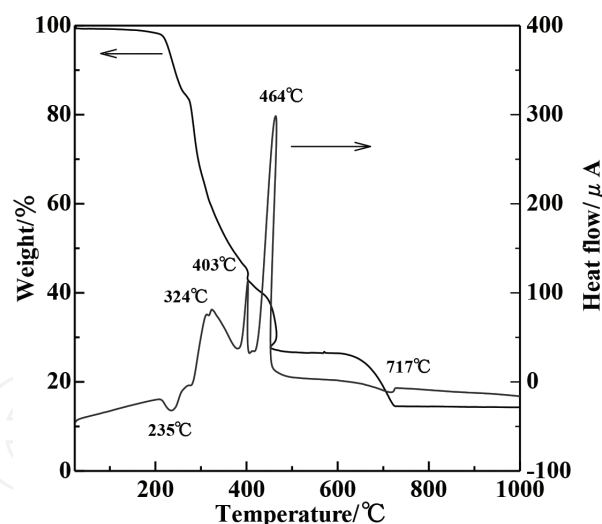


**Figure 3.**  
TG-DTA curves of white compound.

When an aqueous solution of 85 mass% phosphoric acid was directly added to the dibutylammonium salt of the Ca complex with EDTA in ethanol instead of the dibutylammonium diphosphate, the gelation of the mixed solution was observed after several days at ambient temperature. This may be caused by the hydrolysis involving  $\text{Ca}^{2+}$  and  $\text{PO}_4^{3-}$  species due to the copresence of the large amount of water molecules derived from the aqueous solution of phosphoric acid. It is important to note that the present molecular precursor solution does not occur in such a hydrolysis for several months, due to the negligible amount of water in the solution.

## 2.2 Fabrication of the apatite films

Machined commercially pure wrought Ti disks were used as a substrate material. The molecular precursor solution was dropped onto the Ti surface to cover the entire area of the disk. The precursor films formed on the disks were dried at 60°C for 20 min and then fired at 300, 400, 500, 600, and 700°C for 2 h using a furnace in air.

**Figure 4** shows the XRD patterns of the coating films on the substrate at different firing temperatures. No peak could be observed when the precursor films were fired at 300 and 400°C, in the exception of the peaks assignable to Ti. Thus, the heat treatment below 400°C did not produce calcium phosphate crystals on the Ti substrate. Thermal analysis of the molecular precursor gel demonstrated that the decomposition of organic materials occurred at around 360°C and that complete decomposition of organic materials can be achieved at a firing temperature higher than 400°C. By the heat treatment at 500°C, the thickness of the coated film decreased more than that at 300°C. Also, in the XRD patterns of the heat-treated films at 500°C, the peak intensities assignable to Ti substrate increased in comparison with those obtained at 300 and 400°C. These changes in film thicknesses and detection of the Ti substrate are due to the combustion and removal of organic material in the precursor film. The organic materials in the precursor film on the Ti disk disappeared completely at the temperatures in the range 600–700°C.

The CA film formed at a firing temperature at 500°C was almost amorphous, but the films formed at firing temperatures of 600 and 700°C showed a crystalline structure. The greater intensities of the rutile and anatase peaks resulted from heat treatment of the Ti substrate. It is thus suggested that a firing temperature at 600°C is suitable for the production of a thin CA film on the Ti substrate.

The surface of the coating film is quite smooth with no crack nor pinhole.



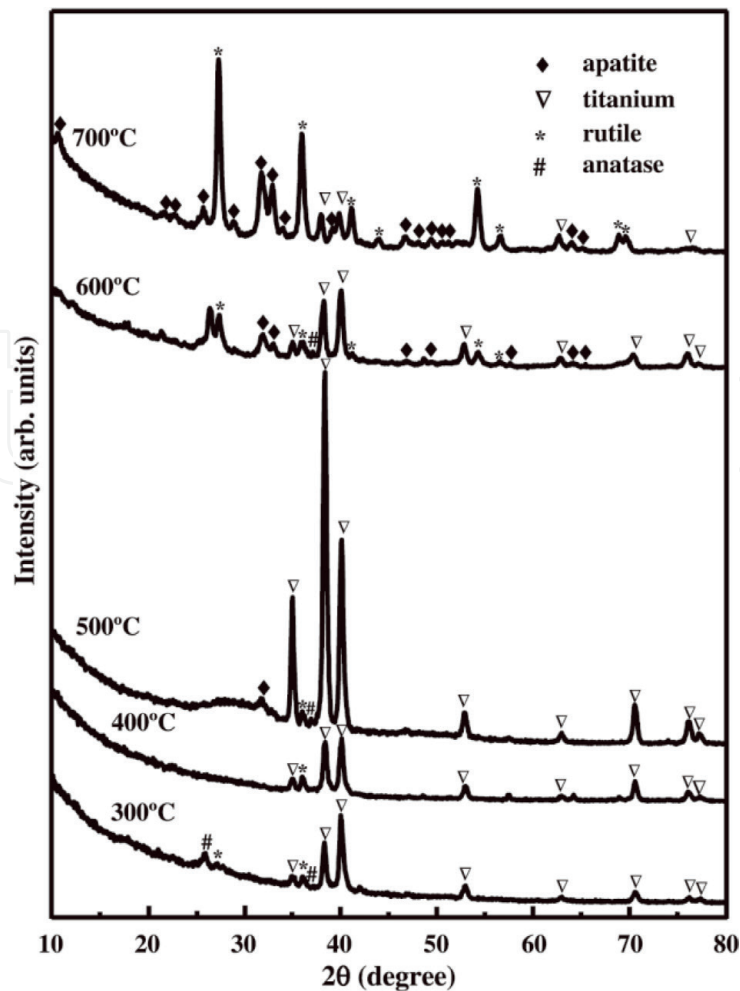


**Figure 4.**  
XRD patterns of CA film firing at several temperatures.

2.3 Characterizations of the fabricated film

**Table 1** lists the changes of film thickness and Ca/P ratio, which was measured by electron probe microanalysis (EPMA), of the coating films fired at 600°C on titanium disk by immersing them in phosphate-buffered saline (PBS, pH = 7.4). It was thus shown that this crystalline apatite film on the Ti substrate is robust to the immersion in PBS. Only a slight crack could be observed after immersion for 7 and 28 days, respectively. No distinct degradation of the deposited coatings was detected. However, the gradual decreases of the Ca/P ratio of the coating film were observed after immersion in PBS. It is suggested that ion exchange reaction between the coating film and PBS occurred gradually via the dissolution/precipitation process.

The tensile bond strength of the coated film onto the Ti substrate was measured to evaluate the degree of adherence. **Table 2** lists the tensile bond strength of CA film on the Ti substrate. The tensile bond strengths of several coating films onto Ti have been reported as follows: 31.9 MPa by the plasma spraying method

Immersion period (day)	0	1	7	28
Coating thickness (μm)	0.44 (0.01)	0.45 (0.01)	0.43 (0.01)	0.45 (0.04)
Ca/P ratio	1.56 (0.04)	1.40 (0.05)	1.41 (0.04)	1.31 (0.05)

**Table 1.**  
Change in thickness of CA film after immersion in PBS.

Substrate	Tensile bond strength (MPa)
Uncoated titanium	42.1 (9.4)
Coated film before PBS immersion	40.2 (5.6)
Coated film after PBS immersion	38.6 (6.3)

**Table 2.**  
*Tensile bond strength of CA film on Ti substrate.*

[30], 8.02–45.82 MPa by ion beam sputtering deposition [31], 59.0 MPa by ion beam dynamic mixing [6], and 32.50 MPa by plasma spraying coating to titanium plasma-sprayed titanium [32], respectively. The bond strength obtained in the present study, 40 MPa, was compatible with these reported values, although it was impossible to obtain the real interfacial bond strength by this method owing to the cohesive failure of the epoxy glue used to fix the samples (**Table 2**).

2.4 Animal experimental and histological evaluation

The CA films on a Ti screw cylinder for animal experiments were coated by using the abovementioned ethanol solution as follows. The Ti screw cylinders were immersed in the molecular precursor solution for 5 min and taken out from the solution slowly. Subsequently, the precursor films that formed on the Ti screw cylinder were dried at 60°C for 20 min and then heat treated at 600°C for 2 h in air using a furnace. The film thickness was approximately 0.16 μm, and the Ca/P ratio was 1.49 ± 0.20. All implants, CA-coated Ti screw cylinder and uncoated Ti screw cylinder, were sterilized in an autoclave before surgery; the implants were inserted into the trabecular bone of rabbits according to a previously used technique [33, 34]. After the implantation for 2, 4, 8, and 12 weeks, no clinical signs of inflammation or adverse tissue reactions were observed at sacrifice. All implants were still in situ at sacrifice. After implantation for 2 weeks, as has been shown in **Figure 5**, the overall trabecular bone response to the two different implant surfaces was almost identical [35]. With progress of implantation time, as for both implants, new bone and remodeling were observed, and no clear differences in bone responses to the two different implants could be seen (as shown in **Figure 6**). Then, besides a descriptive evaluation, the percentage of bone contact was determined for the 4-, 8-, and 12-week specimens. **Table 3** shows the results of the measured percentage of bone-implant contact. At 4 and 8 weeks, no significant difference existed in bone contact between uncoated and CA-coated implants ( $P > 0.05$ ). However, after 12 weeks, statistical analysis revealed that the amount of bone contact to the CA-coated implants was significantly higher than the uncoated titanium implant ( $P < 0.05$ ).

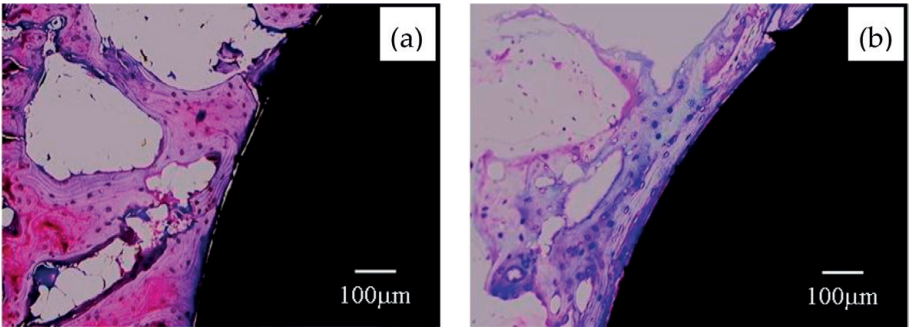


**Figure 5.**  
*Histological appearances of (a) uncoated Ti screw cylinder and (b) CA-coated Ti screw cylinder 2 weeks after implantation.*

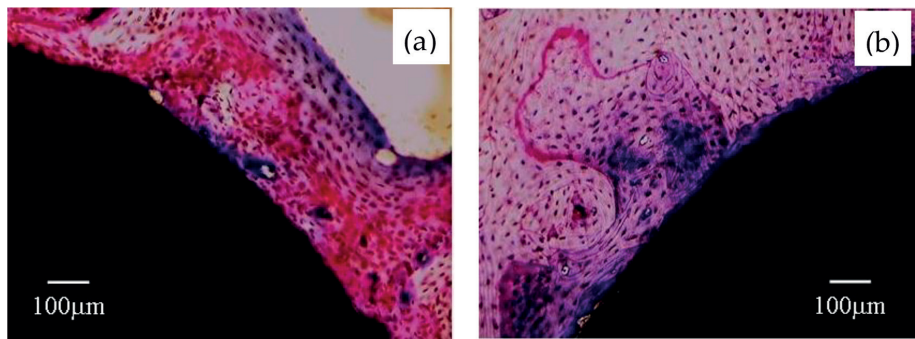


**Figure 6.**  
*Histological appearances of (a) uncoated Ti screw cylinder and (b) CA-coated Ti screw cylinder 12 weeks after implantation.*

	Implantation periods		
	4 weeks	8 weeks	12 weeks
Uncoated	46.4 (16.6)	58.2 (12.4)	71.3 (6.9)
CA coated	47.7 (14.9)	61.8 (10.8)	80.7 (5.6)

*Means connected with vertical lines are not significantly different at  $P > 0.05$ .*

**Table 3.**  
*Percentage of the measured bone-implant contact.*

Wolke and coworkers suggested that 1-µm-thick heat-treated Ca/P sputter coatings on roughened Ti implants appear to be of sufficient thickness to show bioactive properties under in vivo conditions [36]. Our study demonstrated that a CA coating with a thickness of approximately 0.16 µm, which was also inserted into the trabecular bone of the rabbit, has a beneficial effect on the bone response during the healing phase.

From these results, it was suggested that the MPM is promising as the apatite film formation method. Furthermore, this method is useful to fabricate the apatite films homogeneously on various and complicated shapes, e.g., Ti mesh [37].

### 3. Aqueous spray method for apatite coating on titanium substrate

#### 3.1 Preparation of aqueous spray solution

We first prepared a clear solution by blowing CO<sub>2</sub> gas into an aqueous solution of calcium hydroxide [38]. Into the solution, an aqueous solution involving phosphoric acid was then added slowly, and a clear solution could be prepared. Generally, Ca<sup>2+</sup> ion reacts immediately with PO<sub>4</sub><sup>3-</sup> ion in aqueous solution, and calcium phosphate compounds precipitate. However, the finally obtained solution is stable if enough concentration of CO<sub>2</sub> is maintained in the solution. In fact, many crystals of brushite (CaHPO<sub>4</sub>·2H<sub>2</sub>O) deposited when CO<sub>2</sub> in the solution decreased. Therefore, the periodical blowing of CO<sub>2</sub> into the solution can prevent from precipitating such calcium phosphate compounds.

#### 3.2 Fabrication of the apatite films

The CA film on a Ti plate was fabricated by the aqueous spray method and characterized precisely [38]. In the spraying process with a pressure of 0.2 MPa supplied by an air compressor, the mist of the aqueous solution emitted from the nozzle



of an airbrush was vertically collided on a preheated Ti substrate. The thickness of the sprayed film measured by a profilometer and those of the films obtained by heat treatment of the sprayed film at 400–700°C under an Ar gas flow were in the range 1.21–1.40  $\mu\text{m}$ . The well-developed network structure with many round particle was observed on the surface of the sprayed CA film, as has been shown in **Figure 8**. The characteristic network structure of the films fabricated in this present work can be also observed for those formed by the ESD method [17–20]. The size of the network structure found on the surface of the present films (10–15  $\mu\text{m}$ ) was twice as large as those of the films formed by ESD method (5–7  $\mu\text{m}$ ) [39]. The round bulged wall may be formed by spreading of the mist reached on the surface. The round particles (**Figure 7**), which were not observed for the films formed by the ESD method, may be formed by particle growth of the crystal nuclei generated in the sprayed mist during the approach to the substrate and appeared on the film surface. This difference in morphology may be due to the size of the fine drops in the mist and the boiling point of the solvent.

The apatite deposition on the preheated substrate occurs through at least the following four steps. Firstly, spraying of the aqueous solution with compressed air from the nozzle forms fog-like drops of the solution. Secondly, the fog-like drops gradually evaporate due to heat near the substrate, and a continuous increase in ion concentration in the drops occurs during the approach and before contact with the substrate. This step includes the partial removal of  $\text{CO}_2$  gas. In the next step, the concentrated sprayed drops in the mist collide with and spread on the substrate. In the fourth and final step, the spread apatite immediately deposited on the substrate by evaporation of the water molecules in the hydrated ions, and the apatite accumulates by continuous collision of the concentrated sprayed mist.

From the XRD measurement of the sprayed film, it is clear that the apatite structure is easily formed using this method. In addition, the surface morphology of the sprayed film did not change by heat treatment at 400–700°C under an Ar gas flow.

On the other hand, the amount change of the spray solution caused the drastic change of the surface morphologies. **Figure 8** shows the tilt-viewed surface morphologies for **A** whose spray amount and film thickness were 25 mL and 1.3  $\mu\text{m}$  and **B** whose spray amount and film thickness were 5 mL and 0.11  $\mu\text{m}$ , respectively [40]. The image of the thinner-film **B** indicated that the formation of the network structures with round particles occurred as found on the thicker-film **A**, even if the amount of the sprayed solution decreased.

On the basis of these SEM images, **Table 4** also lists the averaged border heights of 10 arbitrarily selected networks. The other two films, **A'** and **B'**, were prepared by heat treating **A** and **B**, respectively, at 600°C for 10 min under Ar gas flow of

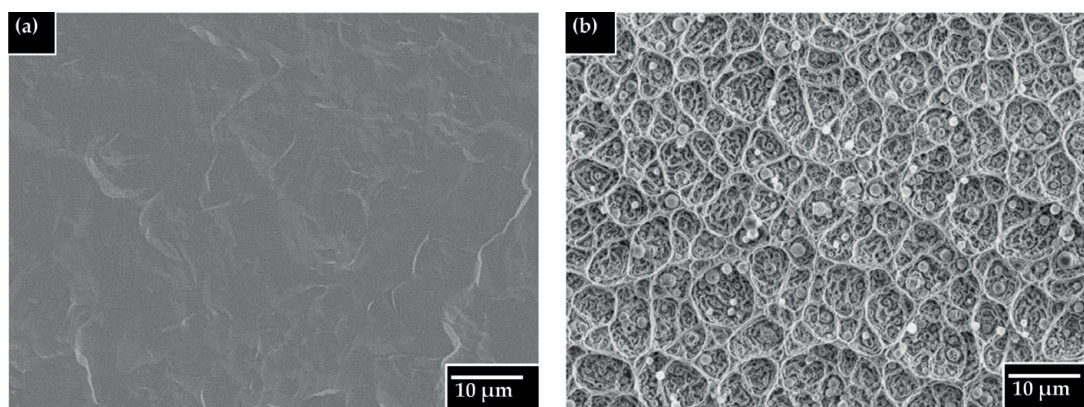


**Figure 7.** Surface morphologies of the (a) Ti substrate and (b) sprayed film (the amount of spray solution is 25 mL).

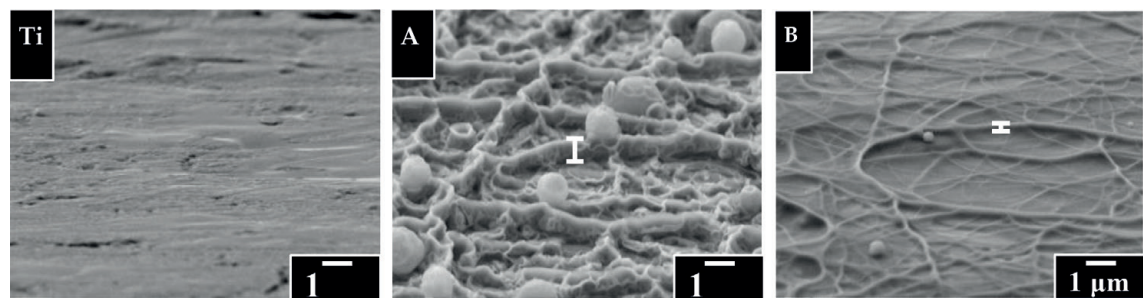


**Figure 8.**  
Tilted-view SEM images of Ti substrate (Ti), spray amount of 25 mL on Ti (A) and spray amount of 5 mL (B). The tilt angle was 85°.

0.5 L min<sup>-1</sup>. The ratios of border height to thickness of A, A', B, and B' were 0.6, 0.8, 2.4, and 2.8, respectively. Thus, the degree of film shrinkage in the vertical direction by thermal densification was larger than that of border height reduction when the films A and B were heat treated in the abovementioned conditions.

3.3 Characterizations of the fabricated film

The results of elemental and Fourier transform infrared (FT-IR) analyses of the powder mechanically collected from the surface of the sprayed film agreed well with those of Ca<sub>10</sub>(PO<sub>4</sub>)<sub>6</sub>(CO<sub>3</sub>)·2CO<sub>2</sub>·3H<sub>2</sub>O.

**Figure 9** shows the FT-IR spectra of the powders collected from the sprayed film before heat treatment and those heat treated at different temperatures. The bands around 1639 and 3435 cm<sup>-1</sup> are likely due to water molecules, but not the hydroxy group. The peak at 2343 cm<sup>-1</sup>, which was observed for both the sprayed film before heat treatment and those heat treated at 400°C and 500°C, can be assigned to the asymmetric stretching mode of the CO<sub>2</sub> molecule [41]; the corresponding peaks for the two films heat treated above 600°C were extremely small. This unexpected behavior of the films heat treated above 600°C may be due to crystallite decay that occurs by elimination of CO<sub>2</sub> molecules that were initially inserted in the apatite skeleton, as shown in the FT-IR spectra.

The shear stresses developed in the sprayed film before heat treatment and the sprayed films heat treated at different temperatures were measured. For the film heat treated at 700°C, the shear stress exceeded the measurable limit, indicating more than 133 MPa based on the maximum load of this instrument (0.50 kg). The shear stress of the sprayed film (21 MPa) is notably larger than the value reported (13 MPa) for an HA film formed on a Ti substrate via plasma spray deposition [42]. The spray solution contains various ions, such as hydroxide, carbonate, and phosphate ions, that may act as bridging ions and can readily form strong chemical bonds at the interface of the Ti substrate and the film. The remarkable decrease in wtthe shear

Notation	Average film thickness	Average border height
	μm	μm
A	1.31 (9)	0.84 (7)
A'	1.21 (4)	0.98 (9)
B	0.12 (2)	0.29 (3)
B'	0.11 (1)	0.31 (6)

**Table 4.**  
Average thicknesses and average border height of network of A, A', B, and B'.

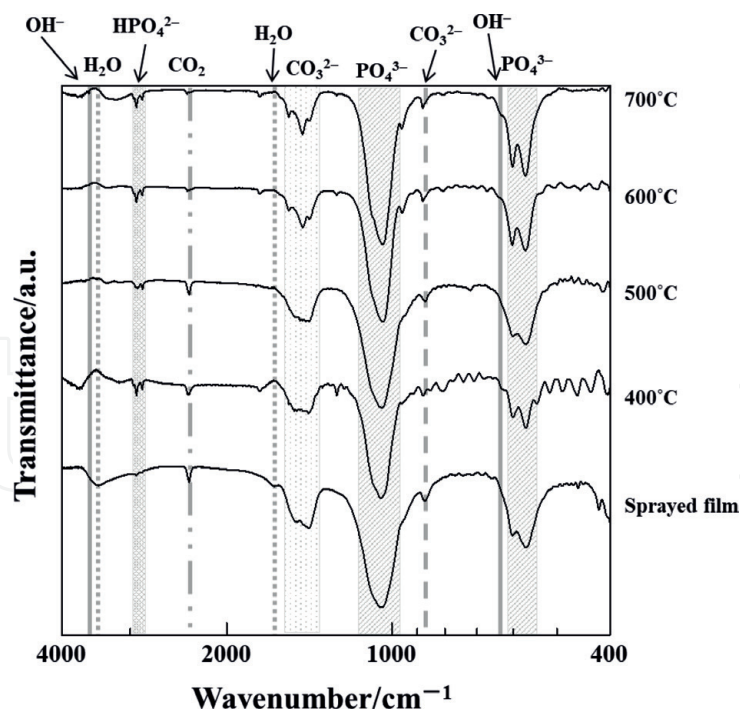


**Figure 9.**  
*FT-IR spectra of the powders obtained from the sprayed film and heat-treated films.*

stresses observed for the films heat treated at 400 and 500°C can also be explained by the following assumption; at these low temperatures, a large amount of CO<sub>2</sub> may be eliminated from the films, because the TG curve shows that CO<sub>2</sub> moieties were removed below 600°C. As a result, the densities of these films formed at low temperatures are relatively low as compared to those obtained at higher temperatures which cause sufficient film densification.

**3.4 Animal experimental and histological evaluation**

Bone responses of Ti implant and CA sprayed on Ti implants, A' and B', were evaluated after implantation into a femoral bone defect in rats [43]. After implantation at 2 weeks, differences in the histopathological appearances of cortical bone formation around the implants revealed new bone formation in all implants (**Figure 10**).

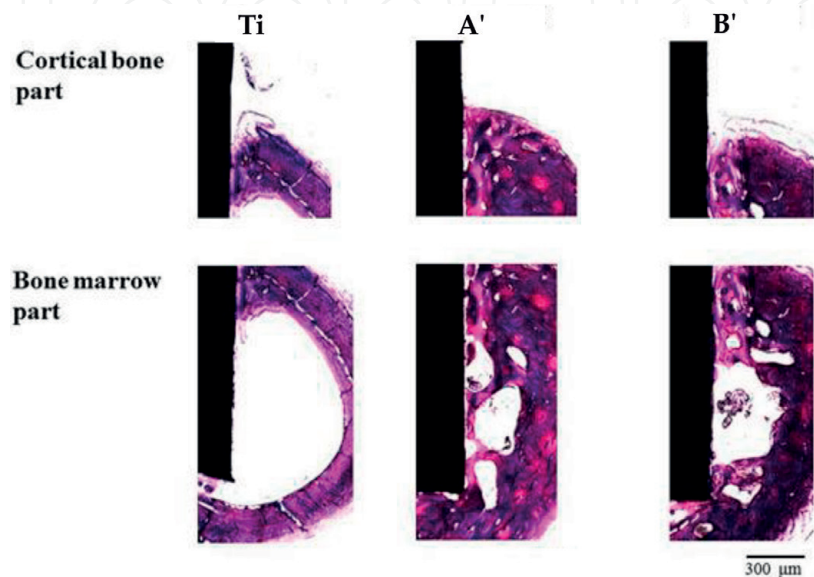


**Figure 10.**  
*Histological appearances of Ti, A' and B', 2 weeks after implantation.*



Notation	Cortical bone part		Bone marrow part	
	2 weeks	4 weeks	2 weeks	4 weeks
Ti	29.7 (14.8)	46.1 (7.6)	22.6 (6.9)	27.6 (14.8)
A'	46.1 (10.0)	64.1 (8.2)	46.5 (9.4)	63.8 (10.2)
B'	41.4 (11.7)	78.7 (4.8)	34.9 (12.3)	72.3 (18.6)

**Table 5.**  
*Measured BIC in cortical bone and bone marrow part of implant specimens.*

Notation	Load/N
Ti	3.3 (0.2)
A'	20.1 (0.7)
B'	23.4 (5.5)

**Table 6.**  
*Measurement push-in loads of implant.*

Haversian canals were observed in **A'** and **B'**, but not in Ti. The bone marrow demonstrated more distinct differences in new bone formation between Ti- and CA-coated specimens. Greater amounts of new bone formation were observed for **A'** and **B'** than for Ti inside the bone marrow. Newly formed bone in bone marrow was trabecular bone, and a part of new bone was formed close to implant materials, **A'** and **B'**.

There were no significant differences in BIC (bone-to-implant contact) in the cortical bone among the three different implants 2 weeks after implantation ( $p > 0.05$ ; **Table 5**). However, 4 weeks after implantation, **A'** and **B'** showed significantly higher BIC than Ti, and BIC was the highest in **B'** ( $p < 0.05$ ). Indeed, BIC was significantly higher for **A'** and **B'** at 4 weeks post-implantation than that at 2 weeks ( $p < 0.05$ ). In the bone marrow, **A'** showed significantly higher BIC than Ti and **B'** at 2 weeks after implantation. At 4 weeks after implantation, BIC of **A'** and **B'** was significantly higher than Ti ( $p < 0.05$ ). No significant differences existed between **A'** and **B'** ( $p > 0.05$ ). BICs of 4 weeks post-implantation were significantly higher than those of 2 weeks for **A'** and **B'** ( $p < 0.05$ ).

CA-coating specimens **A'** and **B'** provided significantly greater amounts of BIC in cortical bone and bone marrow than Ti alone. **B'** was more effective in increasing BIC than **A'**. It is well known that rougher surfaces provide faster and more bone formation [44]. However, the surface roughness did not contribute to an increase of BIC. Mochizuki et al. [40] previously evaluated the attachment, proliferation, and differentiation of osteoblast-like cells on CA-coated Ti. They found that initial attachments of osteoblast-like cells increased due to CA coating and no difference was observed between **A'** and **B'**. On the contrary, cell differentiation was enhanced more on **B'** than on **A'**. They speculated that reduced border heights in the network structure of **B'** were preferred for the spreading of the osteoblast-like cells, and as a result, mineralization would be more accelerated with **B'**. Therefore, higher BIC in the cortical part was obtained for **B'** in the present animal experiments.

The bonding ability of CA-sprayed implant into the bone was examined by push-in tests. **A'** and **B'** showed significantly higher push-in loads than Ti ( $p < 0.05$ ), and there were no significant differences between **A'** and **B'** ( $p > 0.05$ ; **Table 6**). A push-in test was performed to evaluate the bonding between the implant and surrounding bone. Both CA-coating implants produced tighter bonding to the bone than Ti. Surface roughness did not influence the values in push-in

tests. Lin et al. [45] also reported that surface modification with hydroxyapatite nanoparticles increased the push-in values 2 weeks after implantation into the femur of rats. In the present study, we only monitored the peaks at the load-displacement curve. Studies for the failure mode during the push-in test will be necessary to analyze the bonding of CA films to Ti.

#### 4. Conclusion

Using two different Ca complexes, the fabrication of carbonate-apatite films was achieved. The ligands of used complexes play an important role to inhibit the direct reactions of  $\text{Ca}^{2+}$  ion with  $\text{PO}_4^{3-}$  ion in ethanol and aqueous solutions. Furthermore, these ligands of the complexes could be facily removed by usual heat treatment, producing carbonated apatite. The film fabrication by using the ethanol solution, molecular precursor one, involving a Ca complex of EDTA was convenient to form CA films on a Ti plate and screw-type cylinder. The fabricated CA films on a plate have smooth surface and adhered well even if the substrate has a 3D structure such as screw [37]. In addition, a VOC-free coating of CA on a Ti plate was accomplished using an aqueous spray method. The method can easily regulate the thickness and the morphologies of the obtained CA film by changing the amount of spray solution. It was also suggested that the surface morphology of the fabricated CA film by this method is important for the bone reproduction by the CA-coated implant. The CA coating on Ti substrate by the molecular precursor and aqueous spray methods will be useful to clinical application in the field of dentistry.

#### Author details

Chihiro Mochizuki<sup>1</sup>, Mitsunobu Sato<sup>2\*</sup> and Tohru Hayakawa<sup>3</sup>


1 Center for Promotion of Higher Education, Kogakuin University of Technology and Engineering, Tokyo, Japan

2 School of Advanced Engineering, Kogakuin University of Technology and Engineering, Tokyo, Japan

3 School of Dental Medicine, Tsurumi University, Kanagawa, Japan

\*Address all correspondence to: ft10302@ns.kogakuin.ac.jp

#### IntechOpen

© 2018 The Author(s). Licensee IntechOpen. This chapter is distributed under the terms of the Creative Commons Attribution License (<http://creativecommons.org/licenses/by/3.0>), which permits unrestricted use, distribution, and reproduction in any medium, provided the original work is properly cited. 



## References

- [1] Yang Y, Bumgardner JD, Cavin C, Carnes DL, Ong JL. Osteoblast precursor cell attachment on heat-treated calcium phosphate coatings. *Journal of Dental Research*. 2003;**82**:449-453
- [2] Yoshinari M, Ohtsuka Y, Dérand T. Thin hydroxyapatite coating produced by the ion beam dynamic mixing method. *Biomaterials*. 1994;**15**:529-535
- [3] Neuman WF, Neuman MW. *The Chemical Dynamics of Bone Mineral*. Chicago: The University of Chicago Press USA; 1958
- [4] Yoshinari M, Ozeki K, Sumii T. *The Bulletin of Tokyo Dental College*. 1991;**32**:147
- [5] Jansen JA, Wolke JGC, Swann S, Waerden JPCM, Groot K. Application of magnetron sputtering for producing ceramic coatings on implant materials. *Clinical Oral Implants Research*. 1993;**4**:28-34
- [6] Yoshinari M, Klinge B, Dérand T. The biocompatibility (cell culture and histologic study) of hydroxy-apatite-coated implants created by ion beam dynamic mixing. *Clinical Oral Implants Research*. 1996;**7**:96-100
- [7] Jing W, Yang L, Jiyong C, Chenge Z. Chemical gradient in plasma-sprayed HA coatings. *Biomaterials*. 2000;**21**:1339-1343
- [8] Oktar FN, Yetmez M, Agathopoulos A, Lopez Goerne TM, Goller G, Ipeker I, Ferreira JMF. Bond-coating in plasma-sprayed calcium-phosphate coatings. *Journal of Materials Science: Materials in Medicine*. 2006;**17**:1161-1171
- [9] Xu JL, Khor KA. Chemical analysis of silica doped hydroxyapatite biomaterials consolidated by a spark plasma sintering method. *Journal of Inorganic Biochemistry*. 2007;**101**:187-195
- [10] Inagaki M, Kameyama T. *Journal of Plasma and Fusion Research (in Japanese)*. 2007;**83**:595-600
- [11] Klein CPAT, Wolke JGC, Blicke-Hogervorst JMA, Groot KA. Calcium phosphate plasma-sprayed coatings and their stability: An *in vivo* study. *Journal of Biomedical Materials Research*. 1994;**28**:909-917
- [12] Cheang P, Khor KA. Addressing processing problems associated with plasma spraying of hydroxyapatite coatings. *Biomaterials*. 1996;**17**:537-544
- [13] Ogiso M, Yamashita Y, Matsumoto T. Microstructural changes in bone of HA-coated implants. *Journal of Biomedical Materials Research*. 1998;**39**:23-31
- [14] Liu DM, Yang Q, Troczynski T. Sol-gel hydroxyapatite coatings on stainless steel substrates. *Biomaterials*. 2002;**23**:691-698
- [15] Kim HW, Kong YM, Bae CJ, Noh YJ, Kim HE. Sol-gel derived fluor-hydroxyapatite biocoatings on zirconia substrate. *Biomaterials*. 2004;**25**:2919-2969
- [16] Bruce DW, O'Hare D. *Inorganic Materials*. West Sussex: John Wiley & Sons; 1993. 519 p
- [17] Leeuwenburgh SCG, Wolke JGC, Schoonman J, Jansen JA. Electrostatic spray deposition (ESD) of calcium phosphate coatings. *Journal of Biomedical Materials Research*. 2003;**66A**:330-334
- [18] Leeuwenburgh SCG, Wolke JGC, Schoonman J, Jansen JA. Influence of precursor solution parameters on chemical properties of calcium

phosphate coatings prepared using Electrostatic Spray Deposition (ESD). *Biomaterials*. 2004;**25**:641-649

[19] Siebers MC, Walboomers XF, Leeuwenburgh SCG, Wolke JGC, Jansen JA. The influence of the crystallinity of electrostatic spray deposition-derived coatings on osteoblast-like cell behavior, in vitro. *Journal of Biomedical Materials Research*. 2006;**78A**:258-267

[20] Siebers MC, Wolke JGC, Walboomers XF, Leeuwenburgh SCG, Jansen JA. In vivo evaluation of the trabecular bone behavior to porous electrostatic spray deposition-derived calcium phosphate coatings. *Clinical Oral Implants Research*. 2007;**18**:354-361

[21] Zomeren AAV, Kelder EM, Marijnissen JCM, Schoonman J. The production of thin films of  $\text{LiMn}_2\text{O}_4$  by electrospraying. *Journal of Aerosol Science*. 1994;**25**:1229-1235

[22] Siebers MC, Walboomers XF, Leeuwenburgh SCG, Wolke JGC, Jansen JA. Electrostatic spray deposition (ESD) of calcium phosphate coatings, an in vitro study with osteoblast-like cells. *Biomaterials*. 2004;**25**:2019-2027

[23] Sato M, Hara H, Nishide T, Sawada Y. A water-resistant precursor in a wet process for  $\text{TiO}_2$  thin film formation. *Journal of Materials Chemistry*. 1996;**6**:1767-1770

[24] Nishide T, Sato M, Hara H. Crystal structure and optical property of  $\text{TiO}_2$  gels and films prepared from Ti-edta complexes as titania precursors. *Journal of Materials Science*. 2000;**35**:465-469

[25] Sato M, Hara H, Kuritani M, Nishide T. Novel route to  $\text{Co}_3\text{O}_4$  thin films on glass substrates via N-alkyl substituted amine salt of Co(III)-EDTA complex. *Solar Energy Materials & Solar Cells*. 1997;**45**:43-49

[26] Nagai H, Mochizuki C, Hara H, Takano I, Sato M. Enhanced UV-sensitivity of vis-responsive anatase thin films fabricated by using precursor solutions involving Ti complexes. *Solar Energy Materials & Solar Cells*. 2008;**92**:1136-1144

[27] Nagai H, Hasegawa M, Hara H, Mochizuki C, Takano I, Sato M. An important factor controlling the photoreactivity of titania: O-deficiency of anatase thin film. *Journal of Materials Science*. 2008;**43**:6902-6911

[28] Nagai H, Sato M. Heat treatment in molecular precursor method for fabricating metal oxide thin films. In: Czerwinski F, editor. *Heat Treatment—Conventional and Novel Applications*. Rijeka: InTech; 2012. pp. 103-124

[29] Takahashi K, Hayakawa T, Yoshinari M, Hara H, Mochizuki C, Sato M, Nemoto K. Molecular precursor method for thin calcium phosphate coating on titanium. *Thin Solid Films*. 2005;**484**:1-9

[30] Zablotsky M, Meffert R, Mills O, Burgess A, Lancaster D. The macroscopic, microscopic and spectrometric effects of various chemotherapeutic agents on the plasma-sprayed hydroxyapatite-coated implant surface. *Clinical Oral Implants Research*. 1992;**3**:189-198

[31] Ong JL, Lucas LC, Lacefield WR, Rigney ED. Structure, solubility and bond strength of thin calcium phosphate coatings produced by ion beam sputter deposition. *Biomaterials*. 1992;**13**:249-254

[32] Yang Y, Ong JL. Bond strength, compositional, and structural properties of hydroxyapatite coating on Ti,  $\text{ZrO}_2$ -coated Ti, and TPS-coated Ti substrate. *Journal of Biomedical Materials Research*. 2003;**64A**:509-516

- [33] Hayakawa T, Yoshinari M, Kiba H, Yamamoto H, Nemoto K, Jansen JA. Trabecular bond response to surface roughened and calcium phosphate (Ca-P) coated titanium implants. *Biomaterials*. 2002;**23**:1025-1031
- [34] Hayakawa T, Yoshihara M, Nemoto K, Wolke JGC, Jansen JA. Effect of surface roughness and calcium phosphate coating on the implant/bone response. *Clinical Oral Implants Research*. 2000;**11**:296-304
- [35] Hayakawa T, Takahashi K, Yoshinari M, Okada H, Yamamoto H, Sato M, Nemoto K. Trabecular bone response to titanium implants with a thin carbonate-coating apatite coating applied using the molecular precursor method. *International Journal of Oral & Maxillofacial Implants*. 2006;**21**:851-858
- [36] Wolke JGC, van der Waerden JPCM, Schaeken HG, Jansen JA. In vivo dissolution behavior of various RF magnetron-sputtered Ca-P coatings on roughened titanium implants. *Biomaterials*. 2003;**24**:2623-2629
- [37] Hayakawa T, Takahashi K, Okada H, Yoshinari M, Hara H, Mochizuki C, Yamamoto H, Sato M. Effect of thin carbonate-containing apatite (CA) coating of titanium fiber mesh on trabecular bone response. *Journal of Materials Science: Materials in Medicine*. 2008;**19**:2087-2096
- [38] Mochizuki C, Hara H, Takano I, Hayakawa T, Sato M. Application of carbonated apatite coating on a Ti substrate by aqueous spray method. *Materials Science and Engineering: C*. 2013;**33**:951-958
- [39] Siebers MC, Matsuzaki K, Walboomers XF, Leeuwenburgh SCG, Wolke JGC, Jansen JA. Osteoblastic resorption of calcium phosphate coatings applied with electrostatic spray deposition (ESD), in vitro. *Journal of Biomedical Materials Research*. 2005;**74**:570-580
- [40] Mochizuki C, Hara H, Oya K, Aoki S, Hayakawa T, Fujie H, Sato M. Behaviors of MC3T3-E1 cells on carbonated apatite films, with a characteristic network structure, fabricated on a titanium plate by aqueous spray coating. *Materials Science and Engineering: C*. 2014;**39**:245-252
- [41] Sato K, Ikenoya O, Shimazu Y, Aoba T. Carbonation of enamel apatite crystals: Lattice substitutions and surface adsorption. *Journal of Oral Biosciences*. 1999;**41**:61-68
- [42] Zheng XB, Huang MH, Ding CX. Bond strength of plasma-sprayed hydroxyapatite/Ti composite coatings. *Biomaterials*. 2000;**21**:841-849
- [43] Yagi R, Mochizuki C, Sato M, Toyama T, Hirota M, Hayakawa T, Ohkubo C. Characterization and bone response of carbonate-containing apatite-coated titanium implants using an aqueous spray coating. *Materials*. 2017;**10**:1416
- [44] Wennerberg A, Albrektsson T. Effects of titanium surface topography on bone integration: A systematic review. *Clinical Oral Implants Research*. 2009;**20**:172-184
- [45] Lin A, Wang CJ, Kelly J, Gubbi P, Nishimura I. The role of titanium implant surface modification with hydroxyapatite nanoparticles in progressive early bone-implant fixation in vivo. *The International Journal of Oral & Maxillofacial Implants*. 2009;**24**:808-816